Population inversion of $^1G_4$ excited state of Tm^{3+} investigated by means of numerical solutions of the rate equations system in Yb:Tm:Nd:$LiYF_4$ crystal

André Felipe Henriques Librantz,[1] Laércio Gomes,[2,a)] Lilia Coronato Courrol,[3] Izilda Marcia Ranieri,[2] and Sonia Lícia Baldochi[2]
[1]*Departamento de Ciência Exatas, Universidade Nove de Julho (UNINOVE), São Paulo, São Paulo 02111-030, Brazil*
[2]*Centro de Lasers e Aplicações, Instituto de Pesquisas Energéticas e Nucleares (IPEN-CNEN/SP), Butantã, P.O. Box 11049, São Paulo, São Paulo 05422-970, Brazil*
[3]*Departamento de Ciências Exatas e da Terra, Universidade Federal de São Paulo (UNIFESP), Diadema, São Paulo, São Paulo 09972-270, Brazil*

(Received 17 October 2008; accepted 7 April 2009; published online 1 June 2009)

In this work we present the spectroscopic properties of $LiYF_4$ (YLF) single crystals activated with thulium and codoped with ytterbium and neodymium ions. The most important processes that lead to the thulium upconversion emissions in the blue region were identified. A time-resolved luminescence spectroscopy technique was employed to measure the luminescence decays and to determine the most important mechanisms involved in the upconversion process that populates $^1G_4(Tm^{3+})$ excited state. Analysis of the energy transfer processes dynamics using selective pulsed laser excitations in Yb:Tm:Nd, Tm:Nd, and Tm:Yb YLF crystals shows that the energy transfer from Nd^{3+} to Yb^{3+} ions is the mechanism responsible for the enhancement in the blue upconversion efficiency in the Yb:Tm:Nd:YLF when compared with the Yb:Tm system. A study of the energy transfer processes in YLF:Yb:Tm:Nd crystal showed that the $^1G_4$ excited level is mainly populated by a sequence of two nonradiative energy transfers that start well after the Nd^{3+} and Tm^{3+} excitations at 797 nm according to $Nd^{3+}(^4F_{3/2}) \rightarrow Yb^{3+}(^2F_{7/2})$, followed by $Yb^{3+}(^2F_{5/2}) \rightarrow Tm(^3H_4) \rightarrow Tm^{3+}(^1G_4)$. Results of numerical simulation of the rate equations system showed that a population inversion for 481.4 nm laser emission line is attained for a pumping rate threshold of 26 s^{-1}, which is equivalent to an intensity of 880 W cm^{-2} for a continuous laser pumping at 797 nm. On the other hand, a population inversion was not observed for the case of 960 nm (Yb^{3+}) pumping. © *2009 American Institute of Physics*. [DOI: 10.1063/1.3129624]

I. INTRODUCTION

The study of solids doped with thulium ions has received great interest in the past decades due to the numerous applications of these materials. Concerning the thulium emission wavelength, these solids can be used as laser materials[1] for different applications in life sciences,[2] light detection and ranging (LIDAR),[3] and industry or can be applied as the *S*-band Tm-doped fiber amplifier in wavelength-division-multiplexing telecommunication[4] or for optical devices,[5] color displays,[6] and optical memories.[7] Due to the attractive thermomechanical properties, wide transparency, and high optical damage threshold, $LiYF_4$ (YLF) has been studied as laser materials when activated by several RE^{3+} ions, which can easily substitute Y^{3+} ions in a non-center-symmetrical site (S_4 symmetry). YLF has relatively low phonon energy (cutoff of ~650 cm^{-1}) that is an important point in avoiding energy loss by nonradiative relaxation involving the $^1G_4$ and $^3H_4$ excited levels. YLF crystals doped with Tm using Yb^{3+} as a sensitizer has been extensively studied and present two intense emissions around 450 and 475 nm due to the $^1D_2 \rightarrow {}^3F_4$ and $^1G_4 \rightarrow {}^3H_6$ transitions, respectively. Laser emission $^1D_2 \rightarrow {}^3F_4$ at 450 nm was obtained via two-photon pump mechanism at 780 and 650 nm, and laser emission in 475 nm was obtained using a single pump wavelength at 629 nm. The upconversion mechanism was by photon avalanche.[8–12]

In this paper, YLF doped with thulium (Tm^{3+}) ions that are sensitized by neodymium (Nd^{3+}) and ytterbium (Yb^{3+}) was studied, and the multiples processes of energy transfer that occurs when this material is excited around 800 and near 960 nm were inspected, and the transfer rates constants were determined. In light of potential directly diode pumped Tm^{3+}-doped YLF:Yb:Nd crystal lasers, we numerically solved the rate equations for Yb(20 mol %):Tm(0.5 mol %):YLF and Yb(20 mol %):Nd(1 mol %):Tm(0.5 mol %):YLF crystals under cw pumping at 797 nm to determine the population inversion and its dependence on the Nd^{3+} codoping.

II. EXPERIMENTAL PROCEDURE

The rare earth fluorides were prepared from pure oxide powders (Alpha-Johnson Matthey, 99.99%) by hydrofluorination at high temperature in HF atmosphere. The powder was contained in a cylindrical platinum boat, which was inserted in a sealed platinum tube. The LiF-LnF_3 (Ln=Y, Yb, Nd, and Tm) mixture was melted using an open platinum

a)Electronic mail: lgomes@ipen.br.

boat in the same atmosphere with a composition of 1.02 LiF:1 LnF_3. LiF powder (Alpha-Johnson Matthey, 99.9%) was zone-refined before it was added to the mixture. The studied crystals were grown by Czochralski method using automatic diameter control with growth rate of 1.3 mm h^{-1} and rotation rate of 15 rpm for the ⟨100⟩-oriented boule. During the process, the atmosphere inside the Czochralski furnace was composed of Ar (1.4 bar) and CF_4 (0.2 bar). A YLF:Yb:Tm:Nd crystal with 60 mm in length and 20 mm in diameter was obtained from were the samples used in this work were taken.[13] The rare earth concentrations were obtained by inductively coupled plasma-optical emission spectroscopy (ICP-OES) analysis. The following crystals were grown and prepared for the luminescence measurements performed in this work: (i) Yb(20 mol %):Tm(0.5 mol %):Nd(1 mol %):YLF, (ii) Yb(20 mol %):Tm(0.5 mol %):YLF, and (iii) Tm(0.5 mol %):Nd(1 mol %):YLF.

The absorption spectra of all samples were measured in the range of 700–2500 nm at room temperature using a Varian Cary 17D/OLIS spectrophotometer. In the luminescence lifetime measurements, the samples were excited by pulsed laser radiation generated by a tunable optical parametric oscillator-infrared (OPO-IR) pumped (Rainbow from OPOTEK, USA) by the second harmonic of a *Q*-switched Nd: yttrium aluminum garnet laser (Brilliant B from Quantel, France). Laser pulse widths of 4 ns at 960 and 797 nm were used to directly excite the $^2F_{5/2}$ and $^3H_4$ excited states of Yb^{3+} and Tm^{3+}, respectively. Luminescence signals were analyzed by the 0.25 m Kratos monochromator, detected by the EMI S-20 (or S-1) photomultiplier tube (PMT) (response time of 10 ns) or InSb 77 K infrared detector from Judson (response time of ~0.5 μs), and resolved by the EGG Boxcar Processor model 4402 computer interfaced by the general purpose interface bus (GPIB) port. Luminescence lifetime was measured using a digital oscilloscope of 100 MS s^{-1} model TDS 410 from Tektronix interfaced to a microcomputer.

III. EXPERIMENTAL RESULTS

Optical absorption spectra of YLF doped Yb:Tm:Nd crystal have two main absorptions in the near infrared around 960 nm (Yb^{3+}) and around 800 nm due to Nd^{3+} and Tm^{3+} ions. The most intense absorption is near 960 nm due to high concentration of ytterbium in the samples. When YLF crystal containing Tm^{3+} codoped with Yb^{3+} or Yb^{3+} and Nd^{3+} is excited at 797 nm, blue (470–480 nm) Tm^{3+}-emission is observed. Previous results showed that Yb(20 mol %):Tm(0.5 mol %) codoped with Nd^{3+} (~1 mol %) causes an accentuated enhancement in the Tm^{3+} blue emission, indicating that Nd^{3+} ions significantly contribute to the population of the $^1G_4$ excited level that emits around 480 nm.[13] As a minor effect, the population of the $^1G_4$ excited level may interact with $^2F_{5/2}(Yb^{3+})$, exciting the $^1D_2(Tm^{3+})$ level, which emits near 360 and 450 nm. Figure 1 shows the schematic energy diagram levels of Yb/Tm/Nd system. Most of indicated processes will be discussed and proved to be essential for the blue emission upconversion by the luminescence dynamics analysis in the sequence. When the Yb:Tm:Nd or Tm:Nd samples are excited at 792–797 nm the following processes are observed to occur:

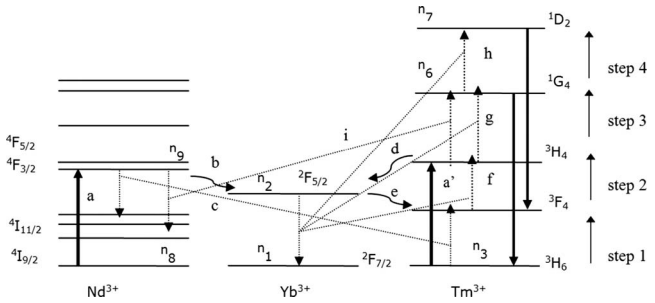

FIG. 1. Energy levels scheme and energy transfer mechanisms of Yb:Tm:Nd system. Solid line (up): 797 nm excitation. Solid lines (down): Tm^{3+} emissions (450 and 480 nm). Dotted lines (up and down): Yb^{3+} emission and cross-relaxation processes.

(a) ground state absorption of $Nd^{3+}(^4I_{9/2}) \rightarrow Nd^{3+}(^4F_{5/2})$,

(a') ground state absorption of $Tm^{3+}(^3H_6) \rightarrow Tm^{3+}(^3H_4)$,

(b) Nd–Yb energy transfer

$$Nd(^4F_{3/2}) + Yb(^2F_{7/2}) \rightarrow Nd(^4I_{11/2}) + Yb(^2F_{5/2}),$$

(c) Nd–Tm energy transfer

$$Nd(^4F_{3/2}) + Tm(^3H_6) \rightarrow Nd(^4I_{15/2}) + Tm(^3F_4),$$

(d) Tm–Yb back-transfer

$$Tm(^3H_4) + Yb(^2F_{7/2}) \rightarrow Tm(^3H_6) + Yb(^2F_{5/2}),$$

(e) Yb × Tm cross-relaxation

$$Yb(^2F_{5/2}) + Tm(^3H_6) \rightarrow Yb(^2F_{7/2}) + Tm(^3H_5),$$

(f) Yb × Tm cross-relaxation

$$Yb(^2F_{5/2}) + Tm(^3F_4) \rightarrow Yb(^2F_{7/2}) + Tm(^3H_4),$$

(g) Yb × Tm cross-relaxation

$$Yb(^2F_{5/2}) + Tm(^3H_4) \rightarrow Yb(^2F_{7/2}) + Tm(^1G_4),$$

(h) Yb × Tm cross-relaxation

$$Yb(^2F_{5/2}) + Tm(^1G_4) \rightarrow Yb(^2F_{7/2}) + Tm(^1D_2),$$

(i) Nd × Tm cross-relaxation

$$Nd(^4F_{3/2}) + Tm(^3H_4) \rightarrow Nd(^4I_{11/2}) + Tm(^1G_4),$$

(p) Tm–Nd energy transfer

$$Tm(^3F_4) + Nd(^4I_{9/2}) \rightarrow Tm(^3H_6) + Nd(^4I_{15/2}),$$

(q) Tm–Nd energy transfer

$$Tm(^3H_4) + Nd(^4I_{9/2}) \rightarrow Tm(^3H_6) + Nd(^4F_{5/2}),$$

(r) Tm × Tm cross-relaxation

$$Tm(^3H_4) + Tm(^3H_6) \rightarrow Tm(^3H_5) + Tm(^3F_4),$$

(s) Tm × Tm cross-relaxation

$$\mathrm{Tm}(^1G_4) + \mathrm{Tm}(^3H_6) \rightarrow \mathrm{Tm}(^3H_5) + \mathrm{Tm}(^3H_4).$$

The luminescence transient of an acceptor state that is indirectly excited by the donor-acceptor (or *D-A*) energy transfer is given by Eq. (1), which has been derived elsewhere[14] for an energy transfer that includes Burshtein (or Inokuti–Hirayama, where $\omega=0$) model due to a dipole-dipole interaction,

$$I_1(t) = I_0\left\{\exp\left(-\frac{t}{\tau_A}\right) - \exp\left(-\frac{t}{\tau_D} - \omega t - \gamma\sqrt{t}\right)\right\}, \qquad (1)$$

where τ_A is the total lifetime of the acceptor (A) excited state and τ_D is the intrinsic lifetime of the donor (D) excited ion. The first term in Eq. (1) gives the luminescence decay of the acceptor, and the second gives the luminescence risetime, which should be equal to the donor total lifetime. The risetime constant was obtained by integration according to Eq. (2) for the case of nonexponential process,

$$\tau = \int_0^\infty \exp\left(-\frac{t}{\tau_d} - \omega t - \gamma\sqrt{t}\right)dt. \qquad (2)$$

For instance, if the diffusion process between donor states dominates the energy transfer mechanism (or $\omega \gg \gamma^2$), the donor decay will be exponential and the acceptor risetime will be exponential. That is the case observed of all the Yb $\rightarrow$Tm transfers in Yb:Tm:Nd and Yb:Tm systems observed in this paper because of the high Yb^{3+} concentration used (20 mol %). In this case, the acceptor luminescence fitting was performed using Eq. (3),

$$I_2(t) = I_0\left\{\exp\left(-\frac{t}{\tau_A}\right) - \exp\left(-\frac{t}{\tau_D}\right)\right\} \quad \text{when} \quad \tau_A > \tau_D$$

or

$$I_2'(t) = I_0\left\{\exp\left(-\frac{t}{\tau_D}\right) - \exp\left(-\frac{t}{\tau_A}\right)\right\} \quad \text{if} \quad \tau_A < \tau_D. \qquad (3)$$

A. Nd–Yb energy transfer

Figure 2(a) shows the $^2F_{5/2}$ upconversion luminescence transient of Yb^{3+} measured at 1000 nm for Yb:Tm:Nd system after pulsed laser excitation at 868 nm with 4 ns of pulse duration. Best fit of Yb^{3+} luminescence transient (1000 nm) was performed using Eq. (1), and $\gamma=476\ \mathrm{s}^{-1/2}$, $\omega=6025\ \mathrm{s}^{-1}$, and $\tau_D=550\ \mu\mathrm{s}$ are the derived energy transfer parameters using a least-squares fit with a correlation coefficient equal to 0.988. The risetime constant of $^2F_{5/2}(Yb^{3+})$ transient luminescence was obtained using the energy transfer parameters (γ and ω) in Eq. (2), giving a risetime constant of $\tau=\tau_{\mathrm{rise}}=\tau_8=7.4\ \mu\mathrm{s}$. For that case, the transfer rate of process (b) was obtained using the relation $b=1/\tau_8 - 1/\tau_{D8}$ that gave the rate constant b a value equal to $1.31\times10^5\ \mathrm{s}^{-1}$ and $\tau_{D8}=\tau_D=550\ \mu\mathrm{s}$ (from the best fit). Figures 2(b) and 2(c) show the luminescence decay of $^4F_{3/2}(Nd^{3+})$ measured at 1052 nm for Yb:Tm:Nd and Tm:Nd systems, respectively. A fast decay of $^4F_{3/2}(Nd^{3+})$ luminescence at 1052 nm was observed for both Yb:Tm:Nd and Tm:Nd systems. Best fit of luminescence decay of $^4F_{3/2}(Nd^{3+})$ was performed using the Burshtein model [second term in Eq. (1)—donor decay], and $\gamma=232\ \mathrm{s}^{-1/2}$, $\omega=5.81\times10^4\ \mathrm{s}^{-1}$, and $\tau_D=550\ \mu\mathrm{s}$ are the derived energy transfer parameters using a least-squares fit for Yb:Tm:Nd system. Best fit parameters obtained for Tm:Nd system were $\gamma=230\ \mathrm{s}^{-1/2}$, $\omega=4.58\times10^4\ \mathrm{s}^{-1}$, and $\tau_D=550\ \mu\mathrm{s}$.

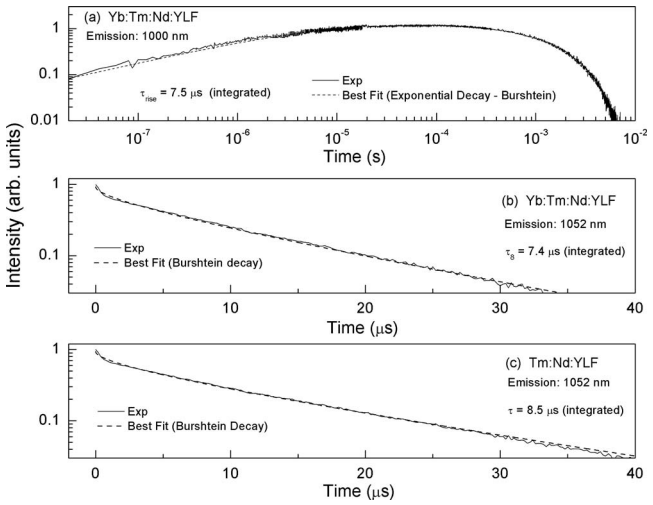

FIG. 2. (a) shows the luminescence transient of $^2F_{5/2}(Yb^{3+})$ excited state measured at 1000 nm after pulsed laser excitation at 868 nm for Yb(20 mol %):Tm(0.5 mol %):Nd(1 mol %):YLF. (b) and (c) show the luminescence decay of $^4F_{3/2}(Nd^{3+})$ level directly excited by pulsed laser excitation at 868 nm for Yb(20):Tm(0.5):Nd(1%) and Tm(0.5 mol %):Nd(1 mol %), respectively. Plots were made in double logarithmic scales to better show the model fitting used (solid lines represent the experimental measurements and dashed lines represent the best fittings). Correlation coefficients equal to 0.988, 0.997, and 0.998 were obtained from best fittings shown in (a)–(c), respectively.

The luminescence lifetime of $^4F_{3/2}(Nd^{3+})$ state was obtained using Eq. (2) that gave $\tau=\tau_8=7.4\ \mu\mathrm{s}$ for Yb:Tm:Nd and $\tau=\tau_8=8.5\ \mu\mathrm{s}$ for Tm:Nd system. This result clearly shows that the energy transfer $\mathrm{Nd}(^4F_{3/2})+\mathrm{Tm}(^4H_6) \rightarrow \mathrm{Nd}(^4I_{15/2})+\mathrm{Tm}(^3F_4)$ [process (c)] observed to occur in Tm:Nd system should be negligible for Yb:Tm:Nd system because the measured lifetime of $^4F_{3/2}$ state ($\tau_8=7.5\ \mu\mathrm{s}$) is equal to the integrated risetime (7.4 μs) verified for the luminescence transient of $^2F_{5/2}(Yb^{3+})$ for Yb:Tm:Nd system. Otherwise, the $^4F_{3/2}$ state would have a shorter lifetime of about 4 μs. The suppression of Nd–Tm transfer observed for Yb:Tm:Nd crystal may be caused by the use of high Yb^{3+} concentration (20 mol %) compared to the Tm^{3+} (0.5 mol %), which increases the random probability that one excited Nd^{3+} ion has to find first an Yb^{3+} ion than a Tm^{3+} besides the fact that Nd $\rightarrow$Tm transfer is a resonant process.

B. Yb–Tm interaction (step 1)

Figure 3(a) shows the $^3F_4$ luminescence transient of Tm^{3+} measured at 1900 nm for Yb:Tm:Nd system after the pulsed laser excitation of Yb^{3+} ions at 960 nm ($E=10$ mJ). This luminescence transient ($^3F_4$) can be better described by $I_3(t)$ given by Eq. (4),

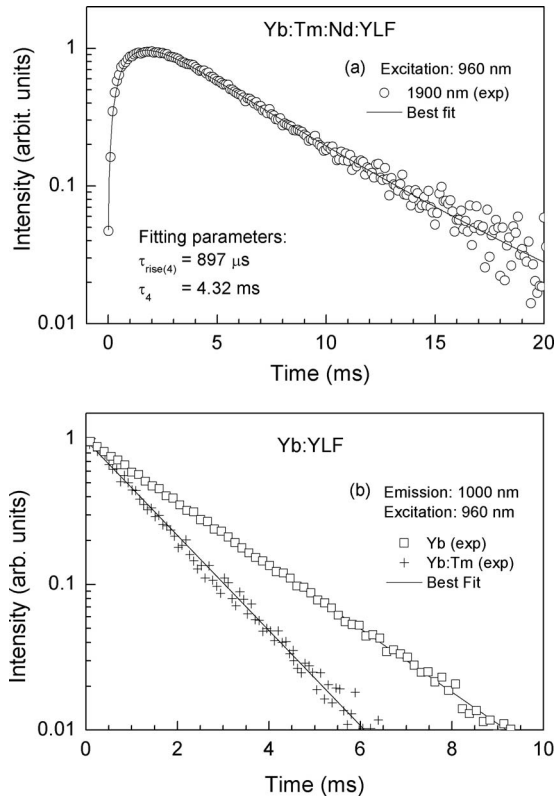

FIG. 3. (a) shows the luminescence transient of $^3F_4(Tm^{3+})$ excited state measured at 1900 nm after pulsed laser excitation at 960 nm for Yb(20 mol %):Tm(0.5 mol %):Nd(1 mol %):YLF (circles represent the experimental data). Plot was made in logarithmic scale of decay to better show the model fitting used. A correlation coefficient equal to 0.985 was obtained for the best fitting represented by the solid line. (b) shows the luminescence decay of Yb^{3+} measured at 1000 nm after the pulsed laser excitation at 960 nm for two systems: Yb(5 mol %):YLF and Yb(20 mol %):Tm(0.5 mol %):YLF, which show τ_2=2 and 1.4 ms, respectively.

$$I_3(t) = I_0\left\{(1-b)\exp\left(-\frac{t}{\tau_A}\right) + b\,\exp\left(-\frac{t}{\tau_A'}\right) - \exp\left(-\frac{t}{\tau_D}\right)\right\}, \quad (4)$$

where I_0 is a constant and b is the fraction of thulium $^3F_4$ ions having an expected (intrinsic) lifetime $\tau_A'=\tau_{D4}$ (~16 ms). Best fit of Tm^{3+} luminescence transient (1900 nm) was performed using Eq. (4), and $\tau_A=\tau_4=4.32$ ms (96%), $\tau_A'=\tau_{D4}=15.5$ ms (4%), $\tau_D=\tau_{rise}=897$ μs are the derived decay constants using a least-squares fit with a correlation coefficient equal to 0.985. The transfer rate constant of process (e) was obtained using the relation $e=1/\tau_{rise}-1/\tau_{D2}$, where $\tau_{rise}=897$ μs and $\tau_{D2}=2$ ms [the intrinsic lifetime of $^2F_{5/2}$ state of Yb^{3+} measured for Yb:YLF crystal shown in Fig. 3(b)]. One gets $e=614$ s^{-1}. The transfer rate constant of process (p) was obtained using the relation $p=1/\tau_4-1/\tau_{D4}$, where $\tau_4=4.32$ ms and $\tau_{D4}=15$ ms (the intrinsic lifetime of $^3F_4$ level[15]). One gets $p=169$ s^{-1}.

Figure 3(b) shows the luminescence decay of Yb(5 mol %):YLF and Yb(20 mol %):Tm(0.5 mol %):YLF measured at 1000 nm after a pulsed laser excitation at 960 nm. Best fittings were done using an exponential decay,

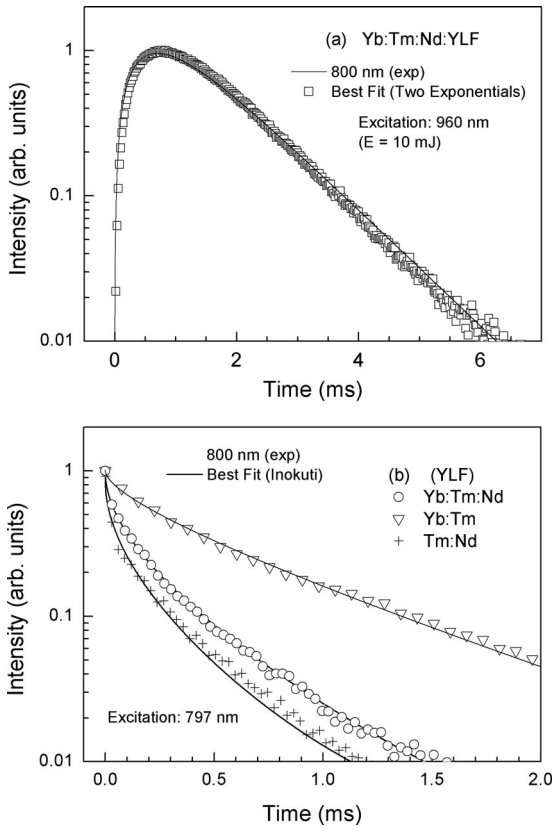

FIG. 4. (a) shows the luminescence transient of $^3H_4(Tm^{3+})$ excited state measured at 800 nm after pulsed laser excitation at 960 nm (E~10 mJ) for Yb(20 mol %):Tm(0.5 mol %):Nd(1 mol %):YLF (experimental data are represented by open squares) and the best fit with a correlation coefficient equal to 0.993 (solid line). (b) shows the luminescence decays of $^3H_4(Tm^{3+})$ level directly excited by pulsed laser excitation at 797 nm (E ~8 mJ) measured for Yb(20 mol %):Tm(0.5 mol %):Nd(1 mol %) (open circles), Yb(20 mol %):Tm(0.5 mol %) (open triangles), and Tm(0.5 mol %):Nd(1 mol %) (crosses) YLF crystals. Plots were made in a logarithmic scale to better show the model fit used (solid lines). The correlation coefficients for the fittings shown in (b) were 0.999, 0.998, and 0.993 for the Yb:Tm:Nd, Yb:Tm, and Tm:Nd systems.

which shows that the $^2F_{5/2}$ level lifetime of Yb^{3+} in Yb:YLF crystal is equal to $\tau_2=\tau_{D2}=2$ ms, while for Yb:Tm and Yb:Tm:Nd crystals the lifetime is 1.4 ms. It is was expected that τ_2 equals 897 μs according to the result in Fig. 3(a). However, one must consider that not all the excited Yb^{3+} ions will interact with Tm^{3+} ions in Yb(20%):Tm(0.5%)-doped system and a fraction of isolated Yb^{3+} excited ions will remain. By this argument, one can consider that the $^2F_{5/2}$ (Yb^{3+}) luminescence exhibited in Fig. 3(b) should be composed of two components: (i) one due to the Yb-luminescence decay dominated by Yb–Tm interaction (55%) having a lifetime of 897 μs and (ii) the second due to the partial isolated Yb^{3+} ions emission with a lifetime of 2 ms (45%). This gives a mean lifetime equal to 1.4 ms for the $^2F_{5/2}$ excited level of Yb^{3+}.

C. Yb–Tm interaction transfer (step 2)

The $^3H_4$ luminescence transients of Tm^{3+} observed at 800 nm that were measured after pulsed laser excitations at 960 and 783 nm are shown in Figs. 4(a) and 4(b), respectively. Pulsed laser excitation at 960 nm (E~10 mJ) was

used to excite the $^3H_4(Tm^{3+})$ upconversion luminescence at 800 nm for Yb:Tm:Nd system as seen in Fig. 4(a). Best fit of Tm^{3+} luminescence transient (800 nm) was performed using $I_2'(t)$ expression given by Eq. (3) (for the case where $\tau_A < \tau_D$) from where best fitting parameters $\tau_A = \tau_{rise(5)} = 470$ μs and $\tau_D = \tau_5 = 1.10$ ms are the derived parameters using a least-squares fit with a correlation coefficient equal to 0.993. One may observe that the $^3H_4$ luminescence risetime ($\sim$470 μs) is longer than the lifetime of $^3H_4$ excited state (τ_5) measured for the Yb:Tm:Nd system, which is equal to 160 μs [see Fig. 4(b)]. However, one must consider the time transient of a *composed donor* obtained by the cross product of $^2F_{5/2}(Yb^{3+})$ luminescence decay (*level 2*) and the $^3F_4(Tm^{3+})$ luminescence transient (*level 4*), which gives the donor risetime $\tau_{rise(24)}^{(donor)} = [1/\tau_2 + 1/\tau_{rise(4)}]^{-1}$ for the case of $^2F_{5/2}(Yb^{3+})$ excitation ($\sim$960 nm) once the decay and risetimes are taken exponentials. Using $\tau_2 = 1.4$ ms and $\tau_{rise(4)} = 897$ μs one gets $\tau_{rise(24)}^{(donor)} = 547$ μs. The energy transfer rate of process (f) can now be calculated using the relation $f = 1/\tau_{rise(5)} - 1/\tau_{rise(24)}^{(donor)} \approx 300$ s^{-1}. By the same argument, one can get $\tau_{decay(24)}^{(donor)} = [1/\tau_2 + 1/\tau_4]^{-1}$. Using $\tau_2 = 1.4$ ms and $\tau_4 = 4.3$ ms (both measured in this work) we get $\tau_{decay(24)}^{(donor)} = 1.06$ ms that is very consistent with the experimental value of $\tau_5 = 1.10$ ms obtained from best fitting in Fig. 4(a).

Best fit of the $^3H_4$ luminescence decay for the Yb:Tm system was done using the second term of Eq. (1) where $\gamma = 28.7$ $s^{-1/2}$, $\omega = 0$, and $\tau_{R5} = 1.08$ ms are the derived parameters from the fitting of the experimental data (triangles) [solid line in Fig. 4(b)]. A decay time of $\tau_{decay(5)}^{(integrated)} = 510$ μs was obtained using Eq. (2). The transfer rate of process (d) could be calculated using the relation $d = 1/\tau_{decay(5)}^{(integrated)} - 1/\tau_{R5} = 1083$ s^{-1}, where $\tau_{decay(5)}^{(integrated)} = 510$ μs (Yb:Tm) and $\tau_{R5} = 1.14$ ms. Results presented in Fig. 4(b) show that the $^3H_4(Tm^{3+})$ excited level is strongly deactivated by Nd^{3+} ions for the Yb:Tm:Nd system [process (q)] similar to the case of Tm:Nd system. Best fit of the $^3H_4$ luminescence decay for the Tm:Nd system was done using the second term in Eq. (1), where $\gamma = 100.7$ $s^{-1/2}$, $\omega = 0$, and $\tau_{R5} = 1.14$ ms are the derived parameters from the fitting of the experimental data (crosses) [solid line in Fig. 4(b)]. A decay time of $\tau_{decay(5)}^{(integrated)} = 118$ μs was obtained using Eq. (2). The rate constant of process (q) was calculated using the relation $q = 1/\tau_{decay(5)}^{(integrated)} - 1/\tau_{R5}$. Using that $\tau_{decay(5)}^{(integrated)} = 118$ μs and $\tau_{R5} = 1.14$ ms (experimental values), one get $q = 7597$ s^{-1}. $Tm(^3H_4):Tm(^3H_6)$ cross-relaxation rate [process (r)] was estimated to be negligible in the case of YLF crystal single doped with 0.5 mol % of thulium because we have verified that the decay time of $^3H_4$ excited state of Tm^{3+} that is equal to 1.21 ms is very close to the radiative lifetime value of 1.2 ms.[15]

D. Yb–Tm interaction (step 3)

The luminescence transient of $^1G_4$ level of Tm^{3+} measured at 480 nm after 797 nm laser pulsed excitation ($E = 9$ mJ) is showed in Fig. 5(a). Best fit of $^1G_4$ luminescence

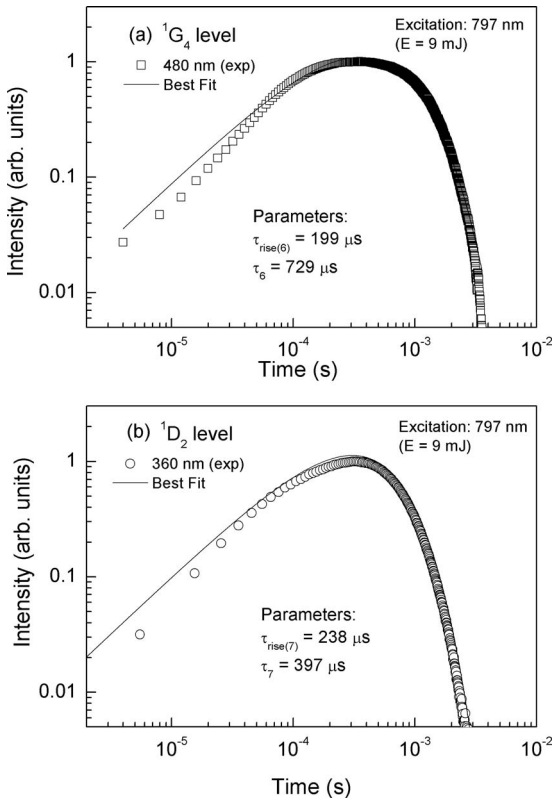

FIG. 5. Decay time of the luminescence transients of $^1G_4$ and $^1D_2$ levels of Tm^{3+} excited by pulsed laser at 797 nm in Yb(20 mol %):Tm(0.5 mol %):Nd (1 mol %):YLF crystal. $^1G_4$ and $^1D_2$ excited states were measured by observing the time dependence of the (a) 480 and (b) 360 nm emissions, respectively. Solid lines represent the best luminescence fittings with correlation coefficients of 0.989 and 0.985, respectively.

transient was performed using $I_2(t)$ expression given by Eq. (3) (for the case where $\tau_A > \tau_D$) from where best fitting parameters $\tau_D = \tau_{rise(6)} = 193$ μs and $\tau_A = \tau_6 = 729$ μs are the derived parameters using a least-squares fit with a correlation coefficient equal to 0.989.

It is noticeable that the $^1G_4$ upconversion luminescence is generated at the expense of a cross interaction between $^2F_{5/2}(Yb^{3+})$ (level 2) and $^3H_4(Tm^{3+})$ (*level 5*) excited levels directly excited by 797 nm pulsed laser excitation. A time transient of the composed donor is obtained by the cross product of $^2F_{5/2}(Yb^{3+})$ luminescence decay (level 2) and the $^3H_4(Tm^{3+})$ luminescence decay (level 5), which gives the composed donor decay time constant $\tau_{decay(25)}^{(donor)} = [1/\tau_2 + 1/\tau_5]^{-1}$ for the Yb:Tm:Nd system. However, two distinct values of composed donors decay constants are obtained and need to be considered. A short decay for the composed donor $\tau_{decay(25)}^{(donor)} = 144$ μs is obtained by considering that the decay time of $^3H_4$ level is dominated by the Tm–Nd interaction where $\tau_5 = 160$ μs was measured for Tm:Nd system. In this case, $\tau_{rise(6)} < \tau_{decay(25)}^{(donor)}$ what makes this process unavailable

On the other hand, if one uses the decay time constant of $^3H_4(Tm^{3+})$ measured for Yb:Tm system ($\tau_5 = 510$ μs), one gets $\tau_{decay(25)}^{(donor)} \sim 374$ μs, which is longer than the measured risetime of $^1G_4$ luminescence transient ($\sim$193 μs). An assumption is made here that most of the Tm^{3+} excited ions

rapidly migrate through $^3H_4$ excited states until get trapped by $Tm^{3+}(^3H_4)\times Yb^{3+}(^2F_{5/2})$ cross interaction such that the effective lifetime of $^3H_4(Tm^{3+})$ level in Yb:Tm:Nd should be equal to the one verified for Yb:Tm system (~510 μs). The transfer rate constant of process (g) was obtained from relation $g=1/\tau_{\text{rise}(6)}-1/\tau_{\text{decay}(25)}^{(\text{donor})}$, where $\tau_{\text{rise}(6)}=193$ μs and $\tau_{\text{deacy}(25)}^{(\text{donor})}=374$ μs, which gave $g=2508$ s^{-1}.

$Tm(^1G_4):Tm(^3H_6)$ cross-relaxation rate [process (s)] was calculated using the decay constant of $^1G_4$ level measured for Yb:Tm:Nd system, where $s=1/\tau_6-1/\tau_{R6}$. Using $\tau_6=729$ μs and the radiative lifetime of $^1G_4(Tm^{3+})$ excited state equal to $\tau_{R6}=770$ μs (Ref. 15), we get $s=73$ s^{-1}.

E. Yb–Tm interaction (step 4)

The luminescence transient of $^1D_2$ level of Tm^{3+} measured at 360 nm after pulsed laser excitation at 797 nm ($E=9$ mJ) is showed in Fig. 5(b). Best fit of $^1G_4$ luminescence transient was performed using $I_2(t)$ expression given by Eq. (3) (for the case where $\tau_A>\tau_D$) from where best fitting parameters $\tau_D=\tau_{\text{rise}(7)}=226$ μs and $\tau_A=\tau_7=397$ μs are the derived parameters using a least-squares fit with a correlation coefficient equal to 0.985. One must note that the $^1D_2$ upconversion luminescence is generated at the expense of a cross interaction between $^2F_{7/2}(Yb^{3+})$ (level 2) and $^1G_4(Tm^{3+})$ (*level 6*) excited states by 797 nm pulsed laser excitation giving the following risetime and decay constant for Yb:Tm:Nd system:

$$\tau_{\text{rise}(26)}^{(\text{donor})}=\left[\frac{1}{\tau_2}+\frac{1}{\tau_{\text{rise}(6)}}\right]^{-1} \quad \text{and} \quad \tau_{\text{decay}(26)}^{(\text{donor})}=\left[\frac{1}{\tau_2}+\frac{1}{\tau_6}\right]^{-1}.$$

The *donor composed* transient has the following calculated rise and decay constants: $\tau_{\text{rise}(26)}^{(\text{donor})}=170$ μs and $\tau_{\text{decay}(26)}^{(\text{donor})}=478$ μs. One must note that the risetime constant measured for the $^1D_2$ level equal to 226 μs is slightly longer than the calculated one from the donor composed transient (170 μs), and therefore it should not contain the energy transfer rate of process (h) we are looking for. Nevertheless, the measured decay time constant of $^1D_2$ state equal to 397 μs is shorter than the calculated value of the donor composed transient equal to 478 μs, allowing to obtain the transfer parameter h (rate) using the relation

$$h=1/\tau_7-1/\tau_{\text{decay}(26)}^{(\text{donor})},$$

which gives $h=426$ s^{-1}.

F. Model for Yb–Tm interaction involving two ions in the excited state

A detailed investigation of the time dependence of the $^1D_2$ and $^1G_4$ upconversion luminescence transients (steps 3 and 4) was carried out by monitoring the upconverted luminescence at 360 and 480 nm as a function of the absorbed excitation energy density by Tm^{3+} ions (N^*). We made a fit to the luminescence transient using two exponentials $I_2(t)$. The rate parameters were obtained in the same way as described in Sec. III D. The result is presented in Table I. Figure 6 exhibits the rate probabilities g [Fig. 6(a)] and h [Fig. 6(b)] as a function of the density of excited Tm^{3+} ions. It can be observed that the rate parameter of process (g) reaches a constant rate when the excited Tm^{3+} ion density reaches a value of 3×10^{18} cm^{-3}, while the rate probability h reaches a constant value for $N^*\sim6\times10^{18}$ cm^{-3} [see Fig. 6(b)]. This behavior suggests the existence of a critical distance R_C between a Tm^{3+} excited ion and an Yb^{3+} indirectly excited by $Nd\rightarrow Yb$ transfer with a time constant of 7.5 μs, comprising the Yb–Tm cross-relaxation [process (g) in this work]. Based on the statistically random separation between the excited Yb^{3+} and Tm^{3+} ions in the crystal lattice, we say that the fraction of excited Yb^{3+} ions, fdR, which has an excited Tm^{3+} ion as the closest neighbor between distance R and $R+dR$, is given by[16]

TABLE I. Parameters used in the rate equation modeling for Yb(20):Tm(0.5):Nd(1):YLF crystal.

Luminescence branching ratio and radiative lifetimes of Tm^{3+} [a]			
Transition	β	τ_R	τ (expt)[b]
Tm^{3+}:			
$^1D_2\rightarrow$		73 μs	74 μs
$^3H_4$	0.17		
$^3F_4$	0.69		
$^3H_6$	0.14		
$^1G_4\rightarrow$		530 μs	730 μs
$^3H_4$	0.17		
$^3F_4$	0.50		
$^3H_6$	0.33		
$^3H_4\rightarrow$		1.2 ms	1.3 ms
$^3F_4$	0.09		
$^3H_6$	0.91		
$^3F_4\rightarrow{}^3H_6$	1	8.8 ms	15 ms
Yb^{3+}:			
$^2F_{5/2}\rightarrow{}^2F_{7/2}$	1	2 ms	1.4 ms
Nd^{3+}:			
$^4F_{3/2}\rightarrow$		538 μs	550 μs
$^4I_{J=15/2,13/2,11/2,9/2}$	1		

Energy transfer rate parameters (expt.)[c]			
Interaction	Process	Rate (s^{-1})	Step
Nd–Yb	(b)	1.31×10^5	···
Tm–Yb	(d)	1083	···
Yb–Tm	(e)	614	1
Yb–Tm	(f)	300	2
Yb–Tm	(g)	2420	3
Yb–Tm	(h)	450	4
Tm–Nd	(p)	169	···
Tm–Nd	(q)	7597	···
Tm–Tm	(r)	~0	···
Tm–Tm	(s)	73	···

[a]Values obtained from the literature (Ref. 15).
[b]Experimental lifetime obtained from best luminescence fitting (in this work).
[c]Experimental transfer rates obtained in this work for Yb(20):Tm(0.5):Nd(1):YLF.

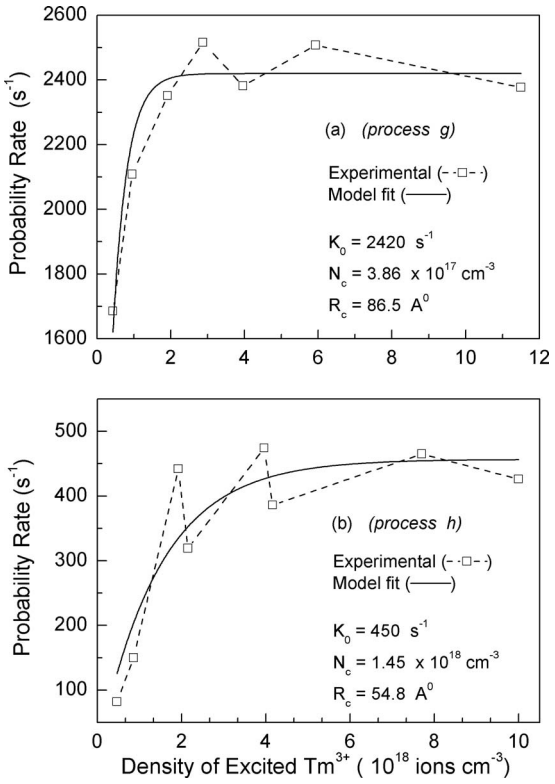

FIG. 6. Rate parameter of $Yb(^2F_{5/2}) \times Tm(^3H_4)$ cross interaction as a function of the experimental excited Tm^{3+} ion density (N^*) obtained by measuring the luminescence transient of the $^1G_4$ level after (pulsed, 4 ns) excitation at 797 nm—which excites also Nd^{3+} ions—shown in (a). (b) exhibits the results of the probability rate of $Yb(^2F_{5/2}) \times Tm(^1G_4)$ cross interaction as a function of N^* (Tm^{3+}) obtained by measuring the luminescence transient of the $^1D_2$ level after excitation (pulsed, 4 ns) at 797 nm. Solid lines represent the best fittings using the proposal model for an ETU involving two ions in the excited state.

$$fdR = 4\pi R^2 N_{\mathrm{Tm}} \frac{N^*}{N_{\mathrm{Tm}}} \left[1 - \frac{N^*}{N_{\mathrm{Tm}}} \right]^{[(4\pi/3)R^3 N_{\mathrm{Tm}} - 2]} dR, \qquad (5)$$

where N^* is the concentration of Tm^{3+} excited ions (cm^{-3}) and N_C is the critical concentration of excited Tm^{3+} ions, which is related to R_C. Integrating Eq. (5) between R_m (the minimum distance between Tm^{3+} ions) and $R=\infty$ yields the transfer efficiency of process (g) [and (h)] as a function of N^* according to

$$\eta = \int_{R_m}^{R_C} fdR \times 1 + \int_{R_C}^{\infty} fdR \times 0 = 1 - \exp(-N_C/N^*), \qquad (6)$$

where we use $\int_{R_C}^{\infty} fdR = \exp(-N_C/N^*)$, which has been determined previously.[16] The observation that Yb–Tm rate parameter dependence on N^* in Figs. 6(a) and 6(b) displays a constant probability rate for higher excitation densities indicates that the Yb–Tm relative efficiency for large values of N^* should be given by $\eta(N^*) = g/K_0$, where K_0 is the rate parameter constant. The solid line in Fig. 6(a) represents the best fit of g rate probability using the model, which gave $N_C = 3.86 \times 10^{17}$ cm^{-3} and $K_0 = 2420$ s^{-1} (or $W_C = 6.26 \times 10^{-15}$ cm^3 s^{-1} using $W_C = K_0/N_C$). Solid line in Fig. 6(b) represents the best fit of the rate probability [process (h)] using the model, which gave $N_C = 1.45 \times 10^{18}$ cm^{-3} and $K_0 = 450$ s^{-1} (or $W_C = 3.1 \times 10^{-16}$ cm^3 s^{-1}). K_0 values should be used in a rate equation system simulating the operation of a laser because under these circumstances, higher excited Tm^{3+} ion densities ($N^* \geq 10^{19}$ cm^{-3}) are usually present. The proposed model for Yb–Tm transfer [processes (g) and (h)] predicts a rate linearly dependent on the N^* for $N^* \ll N_C$, i.e., $K_0 \alpha N^*$, as was previously reported for energy transfer upconversion (ETU) process between two Nd^{3+} ions in the $^4F_{3/2}$ state.[17] Recently it has been demonstrated that ETU rate (s^{-1}) due two Ho^{3+} ions in the $^5I_7$ (or in the $^5I_6$) state of Ho^{3+} in zirconium barium lanthanum aluminum sodium fluoride glasses (ZBLAN) shows a similar dependence on the excitation density of Ho^{3+} ions (cm^{-3}).[18] Detailed investigation of the rate transfer of process (f) has shown a similar rate transfer behavior exhibited (Fig. 6) for process (g). As a consequence, the rate parameter of process (f) (278 s^{-1}) determined in Sec. III C must be considered as a rate constant once it was measured using an excitation density of $\sim 3 \times 10^{18}$ Tm^{3+} ions cm^{-3}.

IV. DISCUSSION

The energy transfer rate parameters (s^{-1}) involved in the Yb:Tm:Nd system, which were obtained in this work, are given in Table I. Process (i) could not be observed using direct excitation of Nd^{3+} and Tm^{3+} ions with 797 nm laser excitation because the $^4F_{3/2}(Nd^{3+})$ excited level rapidly transfers its population to the Yb^{3+} (~ 7.5 μs), so triggering process (g), i.e., process (i) will be considered negligible in Yb:Tm:Nd:YLF crystal. All the optical parameters used in the numerical simulation are listed in Table I.

A. Rate equations for the (Yb^{3+}, Nd^{3+}), Tm^{3+}-codoped YLF system

Figure 1 shows the simplified energy level scheme of Yb:Tm:Nd:YLF system considered for cw diode laser pumping at 797 nm. n_1 and n_2 are the $^2F_{7/2}$ and $^2F_{5/2}$ populations of Yb^{3+}; n_3, n_4, n_5, n_6, and n_7 are the $^3H_6$, $^3F_4$, $^3H_4$, $^1G_4$, and $^1D_2$ populations of Tm^{3+}; and n_8 and n_9 are the $^4I_{9/2}$ and $^4F_{3/2}$ of Nd^{3+}. For Tm^{3+} ion, the $^3F_3$ and the $^3H_5$ excited levels were not considered because they are strongly depopulated by fast multiphonon decay to the next lower lying state. The same argument was used to neglect the $^4I_{11/2}$, $^4I_{13/2}$, $^4I_{15/2}$, and $^4F_{5/2}$ excited levels of Nd^{3+} in the rate equations. The rate equations comprising the model using the fact that $n_1 + n_2 = 0.20$ for an Yb^{3+} concentration of 20 mol %, $n_3 + n_4 + n_5 + n_6 + n_7 = 0.05$ for a Tm^{3+} concentration of 0.5 mol %, and $n_8 + n_9 = 1$ for an Nd^{3+} concentration of 1 mol % are

$$\frac{dn_1}{dt} = \frac{n_2}{\tau_2} + gn_2n_5 + en_2n_3 - dn_1n_5 + fn_2n_4 - bn_1n_8 + hn_2n_6, \qquad (7)$$

$$\frac{dn_2}{dt} = -\frac{n_2}{\tau_2} + dn_1n_5 - gn_2n_5 - en_2n_3 - fn_2n_4 + bn_1n_8 - hn_2n_6, \qquad (8)$$

$$\frac{dn_3}{dt} = -\sigma_{35}n_3\frac{I_P}{h\nu} + \frac{n_4}{\tau_4} + \frac{\beta_{53}}{\tau_{R5}}n_5 + \frac{\beta_{63}}{\tau_{R6}}n_6 + dn_1n_5 - en_2n_3 + pn_4n_8 + qn_5n_8 - rn_3n_5 - sn_3n_6 + \frac{\beta_{73}}{\tau_{R7}}n_7, \quad (9)$$

$$\frac{dn_4}{dt} = -\frac{n_4}{\tau_4} + \frac{\beta_{54}}{\tau_{R5}}n_5 + \frac{\beta_{64}}{\tau_{R6}}n_6 - fn_2n_4 + en_2n_3 - pn_4n_7 + 2rn_3n_5 + sn_3n_6 + \frac{\beta_{74}}{\tau_{R7}}n_7, \quad (10)$$

$$\frac{dn_5}{dt} = \sigma_{35}n_3\frac{I_P}{h\nu} - \frac{n_5}{\tau_5} + \frac{\beta_{65}}{\tau_{R6}}n_6 - dn_1n_5 - gn_2n_5 + fn_2n_4 - rn_3n_5 + \frac{\beta_{75}}{\tau_{R7}}n_7, \quad (11)$$

$$\frac{dn_6}{dt} = -\frac{n_6}{\tau_6} + gn_2n_5 - hn_2n_6, \quad (12)$$

$$\frac{dn_7}{dt} = -\frac{n_7}{\tau_7} + hn_2n_6, \quad (13)$$

$$\frac{dn_8}{dt} = -\sigma_{89}\frac{I_P}{h\nu}n_8 + \frac{n_9}{\tau_9} + bn_1n_9 - pn_4n_8 - qn_5n_8, \quad (14)$$

$$\frac{dn_9}{dt} = \sigma_{89}\frac{I_P}{h\nu}n_8 - \frac{n_9}{\tau_9} - bn_1n_9 + pn_4n_8 + qn_5n_8, \quad (15)$$

where I_P is the pump intensity given in W cm^{-2} and $h\nu$ is the photon energy at 797 nm. β_{ij} represents the luminescence branching ratio and τ_{Ri} is the radiative lifetime of excited states of Tm^{3+} labeled as $i=4$, 5, 6, and 7.

B. Numerical simulation of the rate equation system

Calculations were performed for the Yb(20):Tm(0.5):Nd(1):YLF and Yb(20):Tm(0.5):YLF systems using a computer program developed in SCILAB language, incorporating the Runge–Kutta numerical method. Figure 7 shows the time evolutions of $n_3(t)$ and $n_6(t)$ and Δn, the population inversion $n_6(t)-B_in_3(t)$ of Tm^{3+} after switching the pump laser at $t=0$ (using a pump rate of 200 s^{-1} at 797 nm; B_i is the Boltzmann occupation factor of ground state sublevels). Equilibrium in the populations was obtained after 10 ms in Yb:Tm:Nd:YLF system [see Figs. 7(b) and 7(c) for n_6 and n_3 normalized populations, respectively]. At that stage, the value of Δn was obtained. With the purpose of verifying how the $^4H_6$ multiplet splitting will affect the calculated population inversion, we sketched out the following arguments. The $^3H_6$ ground state of Tm^{3+} has ten sublevels localized at 0 (1), 31 (2), 62 (3), 287 (4), 316 (5), 365 (6), 382 (7), 410 (8), 421 (9), and 436 (10) cm^{-1} (Ref. 19), having Boltzmann occupation factors (B_i) equal to 0.267, 0.228, 0.195, 0.066, 0.056, 0.044, 0.045, 0.035, 0.033, and 0.031, respectively, calculated using $T=300$ K (room temperature). For the purpose of calculating the population inversion, the $^1G_4$ multiplet is located at 21 207 cm^{-1} with a Boltzmann occupation factor of $B_2=1$. Ten emission lines are expected at 471.5 (1), 472.2 (2), 472.9 (3), 478 (4), 478.7 (5), 479.8 (6), 480.2 (7), 480.8 (8), 481.1 (9), and 481.4 nm (10). The population inversion for each $^1G_4 \rightarrow {}^3H_6$ (i) transition will be given by $\Delta n_i = n_6(t)-B_in_3(t)$. We have seen that $\Delta n>0$ for all the emission lines [(1)–(10)]. Figure 8 shows the results obtained by the numerical simulation for cw 797 nm laser pumping. Figure 8(a) shows the population inversion for the emission lines (1), (3), (4), and (10) as a function of the pumping rate. It is observed that the emission line 10 (481.4 nm) has the highest population inversion effect and exhibits the lowest pumping rate threshold of ~26 s^{-1} (that is, equivalent to the pumping intensity of 880 W cm^{-2}). Emission line (1) at 471.5 nm exhibits the lowest population inversion effects and the highest value of pumping rate threshold, ~95 s^{-1}.

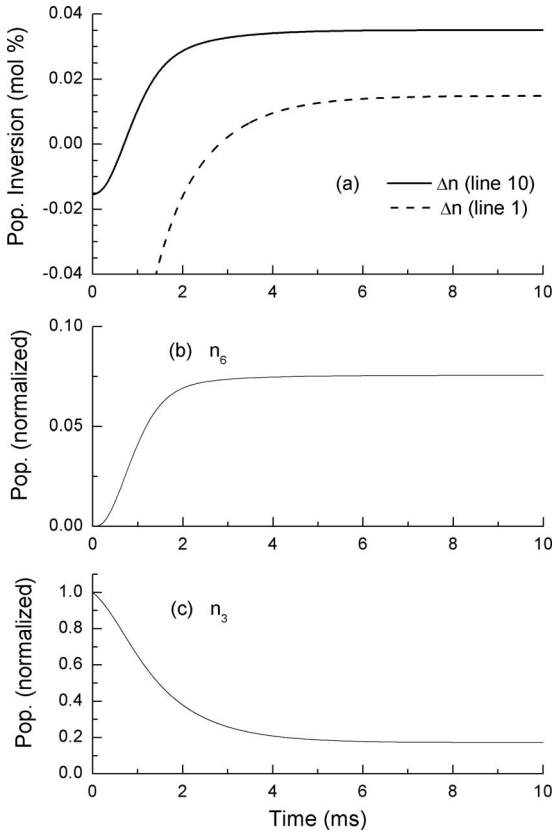

FIG. 7. Calculated evolution of the excited state populations (normalized) of Tm^{3+} obtained by numerical simulation of the rate equations for Yb(20):Tm(0.5):Nd(1):YLF crystal. The simulations were obtained under a continuous pump rate of 200 s^{-1} at 797 nm. Normalized populations $n_6(t)$ and $n_3(t)$ are shown in (b) and (c), respectively. Population inversion was obtained for all laser lines. Gain for the laser lines [(1) and (10)] that emit at 472.5 and 481.4 nm is shown by the dashed and solid lines in (a).

Figure 8(b) shows the population inversion effects obtained for 471.5 (1), 72.9 (3) 478 (4), and 481.4 nm (10) emission lines of Tm^{3+} in Yb:Tm:YLF system as a function of the pump rate (R_P) when considering the [Nd^{3+}] equal to zero in the numerical simulation for cw 797 nm pumping. There it is seen as negative population inversion for most of all laser emissions [results were shown only for the emission lines (1), (3), (4), and (10)]. The pumping rates can be converted to pump intensities I_P (W cm^{-2}) using $I_P = R_P(h\nu)/\sigma_{abs}$, where $\sigma_{abs}(^3H_6 \rightarrow {}^3H_4)=7.3\times10^{-21}$ cm^2 at

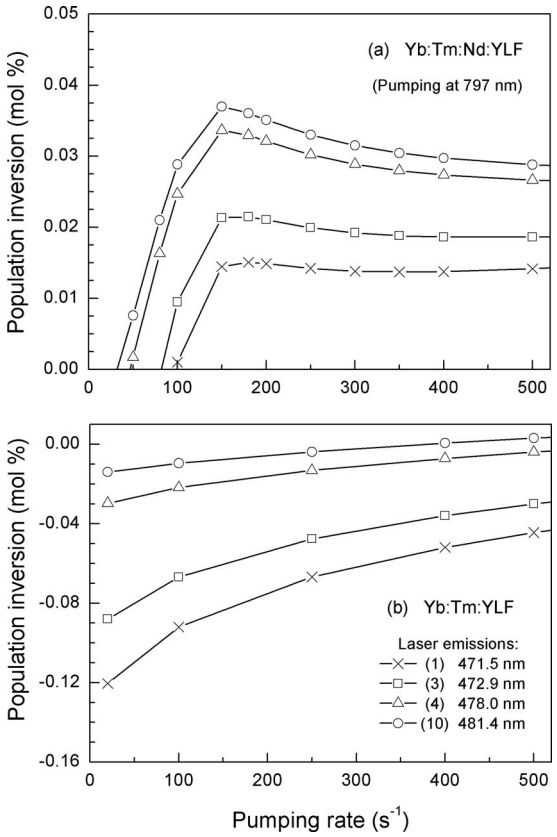

FIG. 8. Results of the population inversions (in mol %) obtained for the emission lines at 471.5 nm (1), 472.9 nm (3), 478 nm (4), and 481.4 nm (10) involved in the $^1G_4 \rightarrow {}^3H_6$ transition of Tm^{3+} are shown in (a) for Yb(20):Tm(0.5):Nd(1):YLF. Results were obtained by numerical simulation for a continuous laser pumping at 797 nm. (b) exhibits the results obtained for the case where the Nd^{3+} concentration is set to zero in the simulation. Note that the 1 mol % corresponds to 1.42×10^{20} ions cm^{-3}.

797 nm, considering the $(\pi+\sigma)$-polarization. The results presented in Fig. 8(a) show that 1 mol % of Nd^{3+} ions leads to a positive Δn values with a low threshold pumping rate of ~ 26 s^{-1} calculated for the laser emission at 481.4 nm.

Figure 9 shows Δn values obtained by using the numerical solutions of the rate equations [Eqs. (7)–(15)] applied to the Yb(20):Tm(0.5):YLF under cw pumping at 960 nm. In this case, negative values of population inversion were obtained for most of the laser emissions involved in the $^1G_4 \rightarrow {}^3H_6$ transition.

V. CONCLUSIONS

Studying the optical properties of YLF doped with Yb/Tm/Nd, it can be concluded that the crystal is efficient and generates blue emission by two-photon process arising from 797 nm excitation, which excites simultaneously Tm^{3+} and Nd^{3+}. A full efficient energy transfer from $Nd^{3+}(^4F_{3/2})$ to $Yb^{3+}(^2F_{5/2})$ was noticed, considering that the Nd^{3+} emission from $^4F_{3/2}$ is very shortened, exhibiting a lifetime of 7.5 μs. The cross-relaxation $Yb(^2F_{5/2}) \times Tm(^3H_4)$ leads to the $^1G_4$ population growth by two order process (or two-photon), while in the case of Yb:Tm system, a $Tm(^3H_4) \rightarrow Yb(^2F_{7/2})$ energy transfer is required first to excite an Yb^{3+} ion with a transfer rate constant of 1083 s^{-1}. This $Tm \rightarrow Yb$ transfer (or

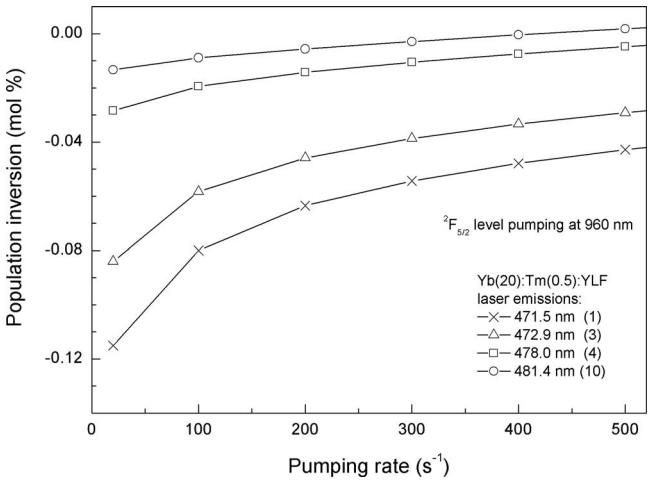

FIG. 9. Results of the population inversions (in mol %) obtained for the emission lines at 471.5 nm (1), 472.9 nm (3), 478 nm (4), and 481.4 nm (10) involved in the $^1G_4 \rightarrow {}^3H_6$ transition of Tm^{3+} are shown for Yb(20):Tm(0.5):Nd(1):YLF system by numerical simulation for a continuous laser pumping at 960 nm (Yb^{3+} excitation).

excitation) rate is much smaller than the $Nd \rightarrow Yb$ transfer rate of 1.31×10^5 s^{-1} observed in the case of Nd-doped (1 mol %) Yb:Tm:YLF.

With all the relevant energy transfer rate parameters measured available, we numerically solved the rate equations for the Yb:Tm:Nd:YLF and Yb:Tm:YLF systems under cw laser pumping at 797 nm. The results established that Yb(20 mol %):Tm(0.5 mol %)-doped YLF crystal that was codoped with 1 mol % of Nd^{3+} showed considerable improvement in the value of Δn as compared to the corresponding Yb:Tm-doped YLF crystal because of strong and fast $Nd \rightarrow Yb$ transfer ($\tau \sim 7.5$ μs), followed by $Yb(^2F_{5/2}) \times Tm(^3H_4)$ cross-relaxation that efficiently populates the upper laser level ($^1G_4$). A threshold pumping rate of 26 s^{-1} was obtained for 481.4 nm emission line of Yb:Tm:Nd:YLF to provide population inversion, $\Delta n > 0$. Considering the population distribution of Stark levels of $^3H_6$ state of Tm^{3+}, the relative gain of each emission line [(1)–(10)] was estimated by means of looking at its Δn_i value. Because it is observed that Δn [(8), (9), and (10)] ~ 7 Δn [(1), (3), and (4)], we claim that Yb(20):Tm(0.5):Nd(1):YLF crystal is suitable for obtaining laser action of ~ 480 nm under cw pumping at 797 nm. It was also seen that the Nd^{3+} doping of 1 mol % is decisive to have gain for blue emission since the gain becomes negative in Yb:Tm system according to the numerical simulation results. Results of numerical simulation showed that Yb(20):Tm(0.5):YLF does not have population inversion for the $^1G_4 \rightarrow {}^3H_6$ transition when pumped by 960 nm cw laser. We have observed also that the $^1D_2$ excited Tm^{3+} level does not have potential gain for the laser emissions at 450 and 360 nm for Yb(20):Tm(0.5):Nd(1):YLF pumped by 797 or 960 nm cw laser.

The numeric method employed in this work to investigate the small signal gain of blue laser emission (~ 480 nm) of Tm^{3+}-doped YLF crystal has been previously applied to describe the laser performance at 2.97 μm of Ho^{3+}:ZBLAN and Ho^{3+}:Pr^{3+}:ZBLAN glass optical fiber lasers (cw) pumped by 1000 nm (Yb-optical fiber laser) and

650 nm (diode laser), respectively, with success.[18,20] It constitutes a useful tool of analyzing the potential laser gain of laser materials and the dopants (activator or sensitizer) concentration optimization.

ACKNOWLEDGMENTS

The authors thank financial support from FAPESP (Grants Nos. 1995/4166-0 and 2000/10986-0) and CNPq.

[1]Y. L. Tang, Y. Yang, X. J. Cheng, and J. Q. Xu, Chin. Opt. Lett. **6**, 44 (2008).
[2]M. K. Tollefson, M. T. Gettman, and I. Frank, J. Urol. (Baltimore) **179**, 365 (2008).
[3]K. Scholle, E. Heumann, and G. Huber, Laser Phys. Lett. **1**, 285 (2004).
[4]Y. Kishi and S. Tanabe, J. Am. Ceram. Soc. **89**, 236 (2006).
[5]L. Tsonev, Opt. Mater. (Amsterdam, Neth.) **30**, 892 (2008).
[6]R. P. Rao, J. Lumin. **113**, 271 (2005).
[7]K. Miura, H. Kawamoto, Y. Kubota, N. Nishimura, and Y. Kita, Central Glass Co. Ltd.
[8]N. P. Barnes, IEEE J. Sel. Top. Quantum Electron. **13**, 435 (2007).
[9]F. Heine, V. Ostroumov, E. Heumann, T. Jensen, G. Huber, and B. H. T. Chai, OSA Proc. Adv. Solid-State Lasers **24**, 77 (1995).
[10]T. Hebert, R. Wannemacher, R. M. Macfarlane, and W. Lenth, Appl. Phys. Lett. **60**, 2592 (1992).
[11]R. Scheps, Prog. Quantum Electron. **20**, 271 (1996).
[12]A. Rapaport, J. Milliez, M. Bass, A. Cassanho, and H. Jenssen, Opt. Express **12**, 5215 (2004).
[13]I. M. Ranieri, L. C. Courrol, A. F. Carvalho, L. Gomes, and S. L. Baldochi, J. Mater. Sci. **42**, 2309 (2007).
[14]L. D. da Vila, L. Gomes, L. V. G. Tarelho, S. J. L. Ribeiro, and Y. Messaddeq, J. Appl. Phys. **93**, 3873 (2003).
[15]C. Li, Y. Guyot, C. Linarés, R. Moncorgé, and M. F. Joubert, OSA Proc. Adv. Solid-State Lasers **15**, 91 (1993).
[16]L. Gomes and F. Luty, Phys. Rev. B **30**, 7194 (1984).
[17]J. Fernandez, R. Balda, M. L. M. Lacha, A. Olega, and J. L. Adam, J. Lumin. **94–95**, 325 (2001).
[18]A. F. H. Librantz, S. D. Jackson, F. H. Jagosich, L. Gomes, G. Poirier, S. J. L. Ribeiro, and Y. Messaddeq, J. Appl. Phys. **101**, 123111 (2007).
[19]H. P. Christensen, Phys. Rev. B **19**, 6573 (1979).
[20]A. F. H. Librantz, S. D. Jackson, L. Gomes, S. J. L. Ribeiro, and Y. Messaddeq, J. Appl. Phys. **103**, 023105 (2008).